Spaceborne Mid- and Far-infrared Observations Improving Nighttime Ice Cloud Property Retrievals

Masanori Saito[1], Ping Yang[1], Xianglei Huang[2], Helen E. Brindley[3], Martin G. Mlynczak[4], and Brian H. Kahn[5]

[1]Laboratory for Atmospheric–oceanic Optics and Remote Sensing, Department of Atmospheric Sciences, Texas A&M University, College Station, TX, USA.

[2]Department of Climate and Space Sciences and Engineering, University of Michigan, Ann Arbor, MI, USA

[3]Space and Atmospheric Physics Group, National Centre for Earth Observation, Imperial College London, London, UK.

[4]NASA Langley Research Center, Hampton, VA, USA.

[5]Jet Propulsion Laboratory, California Institute of Technology, Pasadena, CA, USA.

Corresponding author: Masanori Saito (masa.saito@tamu.edu)

Key Points:

- Spaceborne mid- and far-infrared measurements improve cloud property retrievals in optically thick ice clouds under nighttime conditions
- Temperature and particle habit dependence of ice optical properties at far-infrared wavelengths have substantial impact on the retrievals
- Prior information of subpixel cloud fractions is vital for retrieval accuracy

Abstract

Two upcoming missions are scheduled to provide novel spaceborne observations of upwelling far-infrared spectra. In this study, the accuracy of ice cloud property retrievals using spaceborne mid-to-far-infrared (MIR–FIR) measurements is examined towards a better understanding of retrieval biases and uncertainties. Theoretical sensitivity studies demonstrate that the MIR–FIR spectra are sensitive to ice cloud properties, thereby providing a robust means for retrieving cloud properties under nighttime conditions. However, the temperature dependence of the ice refractive index and relevant ice particle shape models need to be incorporated into the retrieval procedure to avoid systematic biases in inferring cloud optical thickness and effective particle radius. Furthermore, prior information of subpixel cloud fractions is essential to mitigation of substantial systematic retrieval biases due to inconsistent subpixel cloud fractions.

Plain Language Summary

Two upcoming satellite missions will provide the first measurements of spectrally-resolved radiation emitted by the Earth across the so-called ‘far-infrared’ (15-100 microns). We examined the uncertainty of ice cloud property estimations based on simulated mid-to-far-IR spectra observed at the top of the atmosphere. The present results suggest that the aforementioned upcoming satellite missions will offer an opportunity to improve ice cloud property estimations particularly for optically thick clouds. In addition, we demonstrate a pressing need for a better understanding of ice crystal shapes and ice cloud temperature in order to fully exploit the capabilities of the upcoming spaceborne observations.

1 Introduction

Ice clouds cover more than a quarter of the globe (Stubenrauch et al., 2010) and play a pivotal role in the Earth–atmosphere energy system (Stephens et al., 1990; Hong et al., 2016). The spatiotemporal variations of ice cloud properties such as cloud optical thickness (COT) and cloud effective particle radius (CER) are considerable obstacles for a better understanding of cloud radiative forcing (Hong et al., 2009). To monitor ice cloud properties on a global scale, spaceborne passive measurements have been used for decades.

One of two major approaches for ice cloud property retrievals from spaceborne passive observations is the solar reflectance method (Nakajima & King, 1990; Platnick et al., 2001) that utilizes visible and shortwave-infrared (VIS–SWIR) radiation. This approach is robust for COT >0.3 but can be performed only under daytime conditions. Since the ice cloud properties have diurnal variations (Gong et al., 2018; Iwabuchi et al., 2018), the climatologies of the ice cloud properties in the daytime may not be representative at night. Another major approach is the split-window method (Inoue, 1987) based on mid-infrared (MIR; wavelengths 5–15 μm) thermal emission, available day and night. However, this approach is inaccurate for optically thick clouds. Therefore, our current understanding of global ice cloud properties at nighttime is quite limited, which hinders the comprehensive understanding of ice cloud radiative effects.

Two upcoming missions will provide the first-ever satellite observations of upwelling spectral radiance emerging from the Earth, fully or partly covering the far-infrared (FIR; wavelengths 15–100 μm) range. The Polar Radiant Energy in the Far Infrared Experiment (PREFIRE) selected by NASA's Earth Venture program will offer narrow-to-broadband spectral radiance measurements over Arctic regions, covering wavelengths 5–45 μm. The Far-infrared-Outgoing-Radiation Understanding and Monitoring (FORUM), selected as ESA's 9th Earth

Explorer mission, will provide global spaceborne hyperspectral measurements from 100–1600 cm^{-1} (6.25–100 μm), covering the whole FIR and split-window regions.

Between 400–600 cm^{-1}, several semi-transparent FIR "dirty window" bands where water vapor absorption is moderate (Rathke et al., 2002) are useful for ice cloud property retrievals as they have sufficient sensitivity to ice cloud properties (Yang et al., 2003). Most previous studies focus on the sensitivity of ground-based FIR measurements to ice cloud properties (Maestri et al., 2014; Mlynczak et al., 2016; Di Natale et al., 2017), and only a few studies investigate the corresponding sensitivity of upwelling FIR signals (Cox et al., 2010; Bantges et al., 2020). Libois and Blanchet (2017) demonstrate that synergistic measurements of upwelling MIR–FIR radiation significantly reduce the uncertainty in ice cloud property retrievals.

However, several specific error sources affecting FIR-based ice cloud retrievals are known but not well quantified, such as 1) the variation of the ice refractive index with temperature, which has been essentially neglected; 2) the variation of ice optical properties due to complicated ice particle habit variations; and 3) partly cloudy conditions [i.e., subpixel cloud fractions (CF)] which could be common due to the coarse horizontal resolution (12–15 km) of the upcoming spaceborne FIR measurements. Here, we assess the accuracy of ice cloud property retrievals based on synthetic upwelling MIR–FIR window simulations with a focus on these three potential error sources.

Section 2 describes methods for the ice cloud retrievals and uncertainty evaluation. Section 3 shows results and discussions. Section 4 summarizes the major findings of this study.

2 Methods

2.1 Ice cloud bulk optical properties at FIR wavelengths

We consider spaceborne MIR split-window band (M01–M03) and FIR dirty window band (F01–F05) measurements. Table 1 lists selected spectral bands and their typical measurement noise estimated from the goal specification of the FORUM sounding instrument (0.4 and 1.0 mW m^{-2} sr^{-1} cm^{-1} from 200–800 cm^{-1} and 800–1600 cm^{-1}, respectively, Ridolfi et al., 2020) with a reference temperature of 230 K. The spectral response function (SRF) is assumed to be a Gaussian distribution with the full width at half-maximum (FWHM) of 0.36 cm^{-1} for FORUM- and 0.84 μm for PREFIRE-like simulations. Bulk optical properties of ice clouds are calculated for each spectral band using a gamma particle size distribution with an effective variance of 0.1 (e.g., Platnick et al., 2017). We consider several ice particle habits with severely roughened particle surfaces, including the 8-column aggregate (CAGG), 10-plate aggregate (PAGG), solid bullet rosette (SBUL), solid column (SCOL), and two-habit model (THM) (Yang et al., 2013; Loeb et al., 2018). These ice models consider the temperature dependence of the ice refractive index (Iwabuchi & Yang, 2011).

Figure 1 shows the simulated bulk ice optical properties in two FORUM-like FIR bands (F02 and F05) for various temperatures and ice particle habits. The impact of the temperature dependence of the ice refractive index on the bulk ice optical properties in the FIR domain is apparent for all crystal sizes and is more prominent than in the MIR domain (Iwabuchi et al., 2014). In particular, the bulk single-scattering albedo (SSA) of ice crystals shows substantial variations with temperature (Fig. 1b), which, in band F02, is almost as large as its variation with CER. All bulk ice optical properties also vary noticeably with ice particle habit at the FIR bands (Figs. 1d–f).

Table 1. Spectral band information and the measurement noise assumed in this study.

Bands	M01	M02	M03	F01	F02	F03	F04	F05
Center wavelengths (μm)	8.56	11.02	12.03	17.87	20.13	24.38	27.39	41.93
Measurement noise (K)	2.4	1.3	1.2	0.5	0.5	0.5	0.6	1.0

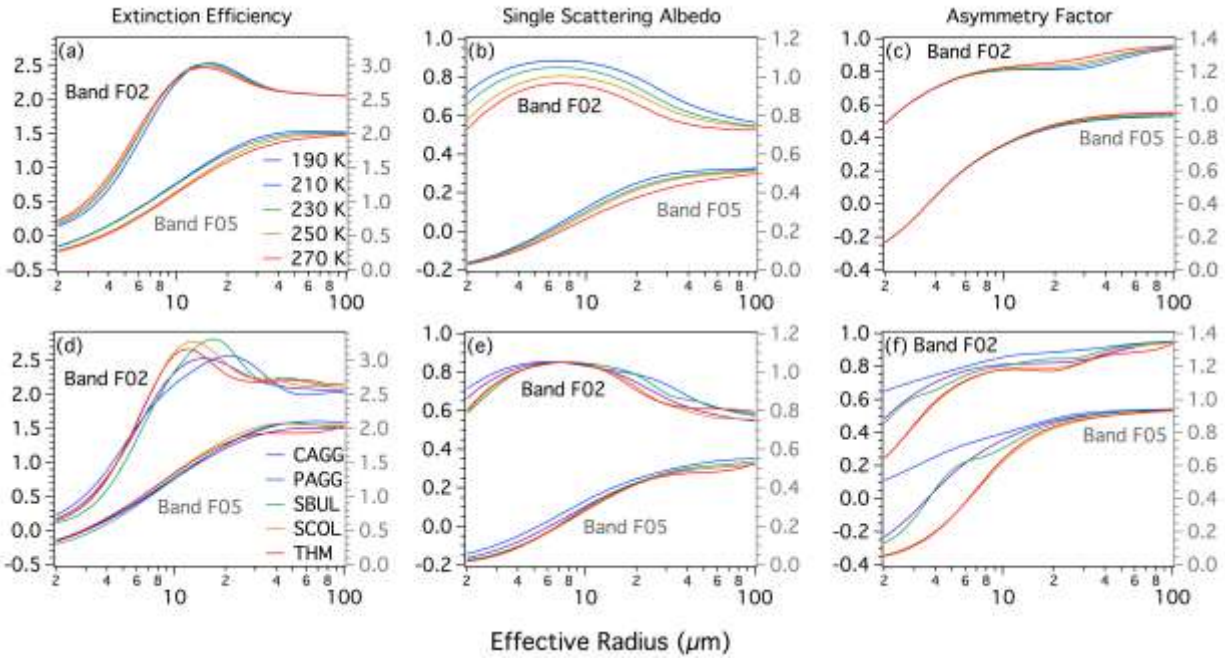

Figure 1. (a–c) The temperature dependence (190–270 K) and (d–f) ice particle habit dependence (CAGG, PAGG, SBUL, SCOL, and THM) of the bulk (left column) extinction efficiency, (center column) single-scattering albedo, and (right column) asymmetry factor of ice clouds in two FORUM-like FIR bands (F02 and F05 corresponding to left and right axes), for CERs shown on

the x-axis. The ice particle habit in upper panels is CAGG, and a reference temperature of the ice refractive index in lower panels is 230 K.

2.2 A parameterized brightness temperature model

In general, a computationally efficient cloud retrieval algorithm is required for operational use due to the large amount of data. Therefore, a rigorous but computationally expensive radiative transfer model (RTM) is not always useful. We use a computationally efficient yet reasonably accurate parameterized RTM (see Appendix in Saito et al., 2020) to simulate brightness temperatures (T_{BT}) in MIR and FIR window bands. The RTM is conceptualized by considering the radiative contribution from the surface, cloud, and atmosphere below and above the cloud. The layer atmospheric gas transmissivity and radiation are computed with parameterized gas absorption coefficients based on Sekiguchi and Nakajima (2008) and specified vertical profiles of pressure, temperature, and water vapor. The T_{BT} in each band is calculated as

$$T_{\mathrm{BT}} = B^{-1}\left[I_{\mathrm{TOA}}\left(\mu, f, W, \varepsilon_{\mathrm{sfc}}, T_{\mathrm{sfc}}, T_{\mathrm{bas}}, T_{\mathrm{top}}, T_{\mathrm{opt}}, \tau_{\mathrm{VIS}}, R_{\mathrm{e}}\right)\right], \quad (1)$$

where B(T) is Planck's function, and the TOA radiance is a function of the cosine of viewing zenith angle (μ), subpixel CF (f), total precipitable water (W), surface emissivity ($\varepsilon_{\mathrm{sfc}}$), surface temperature ($T_{\mathrm{sfc}}$), cloud base temperature (T_{bas}), cloud top temperature (T_{top}), a reference temperature of the ice refractive index (T_{opt}), COT defined at wavelength 0.55 μm (τ_{VIS}), and CER (R_{e}). Cloud geometrical thickness (ΔH) is parameterized as $\Delta H = \min\left[G\sqrt{\tau_{\mathrm{VIS}}}, 6\right]$, where G = 2 km (Iwabuchi et al., 2014; Saito et al., 2020). The T_{bas} is obtained from T_{top}, ΔH and a given atmospheric temperature profile. We assume T_{opt} simply to be (T_{top} + T_{bas})/2.

139 2.3 The retrieval method

140 The retrievals are based on the optimal estimation method (Rodgers, 2000). The state
141 vector (**x**), measurement vector (**y**), and model parameter vector (**b**) are

$$\mathbf{x} = \begin{pmatrix} \ln \tau_{\mathrm{VIS}} \\ \ln R_{\mathrm{e}} \\ T_{\mathrm{top}} \\ T_{\mathrm{sfc}} \end{pmatrix}, \qquad \mathbf{y} = \begin{pmatrix} T_{\mathrm{BT,M01}} \\ T_{\mathrm{BT,M02}} \\ T_{\mathrm{BT,M03}} \\ T_{\mathrm{BT,F01}} \\ T_{\mathrm{BT,F02}} \\ T_{\mathrm{BT,F03}} \\ T_{\mathrm{BT,F04}} \\ T_{\mathrm{BT,F05}} \end{pmatrix}, \text{ and } \mathbf{b} = \begin{pmatrix} T_{\mathrm{opt}} \\ \Delta H \\ W \\ \varepsilon_{\mathrm{T01}} \\ \vdots \\ \varepsilon_{\mathrm{F05}} \end{pmatrix}. \tag{2}$$

143 The measurement signals are simulated as

$$\mathbf{y} = \mathbf{F}(\mathbf{x}, \mathbf{b}, \mu, f) + \mathbf{e}\,, \tag{3}$$

145 where **F** is the forward model and **e** is the measurement–model error. An optimal solution of **x** is
146 obtained by minimizing the cost function given by

$$J = (\mathbf{x} - \mathbf{x_a})^{\mathrm{T}} \mathbf{S}_a^{-1} (\mathbf{x} - \mathbf{x_a}) + [\mathbf{y} - \mathbf{F}(\mathbf{x}, \mathbf{b}, \mu)]^{\mathrm{T}} \mathbf{S}_y^{-1} [\mathbf{y} - \mathbf{F}(\mathbf{x}, \mathbf{b}, \mu)], \tag{4}$$

148 where $\mathbf{x}_{\mathrm{a}}$ is an *a priori* vector, and $\mathbf{S}_{\mathrm{a}}$ is the error covariance matrix of the *a priori*. This study
149 assumes *a priori* values $\tau_{\mathrm{VIS}} = 3$ and $R_{\mathrm{e}} = 15$ μm (Kahn et al., 2014), and large *a priori*
150 uncertainty of $\ln \tau_{\mathrm{VIS}}$ and $\ln R_{\mathrm{e}}$ (= 2.3, respectively), indicating a small contribution of the prior
151 information to the retrievals. For T_{top} and T_{sfc}, we assume that prior information from other
152 satellite-based products is available (Wan & Li, 1997; Menzel et al., 2008), and the *a priori*
153 uncertainties are assumed to be 4 K for T_{top} and 1 K for T_{sfc}, according to the typical uncertainty
154 in these operational products.

155 The covariance matrix of the measurement–model error ($\mathbf{S}_{\mathrm{y}}$) is given by

$$\mathbf{S}_{y} = \mathbf{S}_{y,obs} + \mathbf{S}_{y,fwd} + \mathbf{K}_{b}\mathbf{S}_{b}\mathbf{K}_{b}^{T}, \quad (5)$$

where $\mathbf{S}_{y,obs}$ and $\mathbf{S}_{y,fwd}$ denote the measurement noise and forward model error, respectively. The third term in the right-hand-side of Eq. (5) describes the forward model uncertainty associated with the model parameter error ($\mathbf{S}_{b}$), where $\mathbf{K}_{b}$ is a Jacobian matrix with respect to the model parameters. This study assumes $\mathbf{S}_{a}$, $\mathbf{S}_{y,obs}$, and $\mathbf{S}_{y,fwd}$ to be diagonal matrices.

Table 2 describes the model parameters and their uncertainties assumed in this study. In the retrieval error analysis (Section 2.4), we consider two atmospheric scenarios (tropics and polar regions) to investigate the feasibility of applying the proposed retrieval approach to a global analysis. The climatology of the cirrus T_{top} is ~203 K in the tropics and ~213 K in the polar regions according to one year of spaceborne lidar measurements (Sassen et al., 2008). Typical values and uncertainties of the surface type, temperature, emissivity, and total precipitable water in these two regions (e.g., Feldman et al., 2014; Bellisario et al, 2017) are used in this study.

Table 2. Assumed states, model parameters, and their uncertainties.

Variables	Assumed values		Assumed errors (±1σ)
	Tropical scenario	Polar scenario	
T_{top}	203 (K)	213 (K)	4.0 (K)
T_{sfc}	300 (K)	258 (K)	1.0 (K)
T_{opt}	Defined		6.0 (K)
ΔH	Defined		1.0 (km)
W	50.0 (mm)	2.0 (mm)	15.0 (mm) tropical scenario 1.0 (mm) polar scenario
ε	Ocean, Huang et al. (2016)	Snow, Chen et al. (2014)	0.005 (All types, MIR band) 0.01 (Ocean, FIR band) 0.05 (Snow, FIR band)

Additional errors may be caused when the forward model assumptions are inconsistent with actual atmospheric and cloud states. For example, single-layer and ice-phase cloud assumptions may cause retrieval biases in reality due to the presence of multilayer mixed-phase clouds (Kahn et al., 2015; Guillaume et al., 2019). Also, water vapor absorption in the FIR domain could have some uncertainty (Mlawer et al., 2019). However, their treatment is beyond the scope of this study.

2.4 Retrieval error analysis

We evaluate the mean bias error (MBE) and the root-mean-square error (RMSE) of ice cloud property retrievals based on noise-synthetic FORUM- and PREFIRE-like simulations

(Iwabuchi et al., 2014). MBE is important in terms of the climatology of ice cloud properties because a large MBE skews the probability density distributions of the ice cloud properties. RMSE is critical for pixel-by-pixel ice cloud property retrievals. We do not focus on information content and uncertainties of the ice cloud property retrievals, which have been extensively investigated by Libois and Blanchet (2017).

The retrieval error analysis is performed based on FORUM- and PREFIRE-like simulations considering two measurement cases: 1) MIR measurements and 2) synergistic MIR–FIR measurements. By comparing these measurement cases, we evaluate how much incorporating spaceborne FIR measurements is likely to improve existing ice cloud property retrievals.

3 Results and discussion

3.1 Retrieval performance of ice cloud property retrievals

Figure 2 shows the MBE and RMSE of the retrievals based on synthetic FORUM simulations for both atmospheric scenarios and PREFIRE simulations for the polar scenario. In all cases, a subpixel CF of 100% and an ice particle habit of CAGG is assumed. The FORUM-like MIR-based ice cloud property retrieval can perform well in optically thin clouds, which is consistent with previous studies (e.g., Cooper & Garrett, 2010) but show a large MBE and RMSE in COT and CER retrievals for optically thick (COT > ~8) clouds. In the FORUM-like MIR–FIR retrieval, the MBEs of COT and CER are remarkably small for COT from 0.3–30 and CER from 5–80 μm, which generally covers the realistic cloud retrieval range captured by retrieval methods using VIS–NIR observations. The RMSEs also markedly decrease for optically thick clouds. Note that the retrieval uncertainty in optically thin ice clouds mainly relies on the measurement noise in

the MIR bands. If the MIR measurement noise is as small as the MODIS counterpart, the MBEs become close to zero for COT $\geq$0.1.

The FORUM-like MIR-based retrievals for the polar scenario show a substantially larger MBE than for the tropical scenario, especially for CER retrievals, due to the small thermal contrast between the cloud top and surface. Indeed, the small MBE domain shrinks to COT from 0.5–6 and CER from 15–30 μm in the MIR-based retrievals while in the FORUM-like MIR–FIR-based retrievals, the MBE is small for COT from 0.8–30 and CER from 5–80 μm. The polar simulations show that ice cloud property retrievals for COT < 0.5 are difficult even using MIR–FIR channels. This is because the upwelling FIR radiance contains a substantial contribution from the atmosphere below the cloud when the cloud is optically thin and is very sensitive to column water vapor under the dry atmospheric conditions (Turner & Mlawer, 2010). In addition, the MIR–FIR-based retrievals become unstable when COT <0.8 due to the non-uniqueness of the solution. However, adding FIR measurements enlarges the region of small MBE for both atmospheric scenarios, especially for optically thick clouds.

The PREFIRE-like MIR-based and MIR–FIR-based COT retrievals show similar performance to that seen in the FORUM-like retrievals for the polar scenario. The MIR–FIR-based CER retrievals show slight improvement for optically thick clouds compared to the MIR-based counterparts. As long as water vapor absorption above ice clouds is small, the FIR window measurements reduce MBE and RMSE of ice cloud property retrievals in optically thick clouds. Since actual PREFIRE SRFs are not available, a Gaussian shape is assumed in the PREFIRE-like retrieval simulations, which potentially might underestimate the retrieval performance especially for the CER retrievals because the Gaussian shape usually has a longer tail than typical SRFs and therefore can include more water vapor line absorption.

Thus, the MIR–FIR-based ice cloud retrievals reduce MBEs and RMSEs of ice cloud property retrievals for optically thick clouds compared to the MIR-based ice cloud retrievals. This implies that the MIR–FIR measurements could offer a means to compensate for the unavailability of VIS–NIR-based retrievals of optically thick ice clouds at night, especially in the tropics.

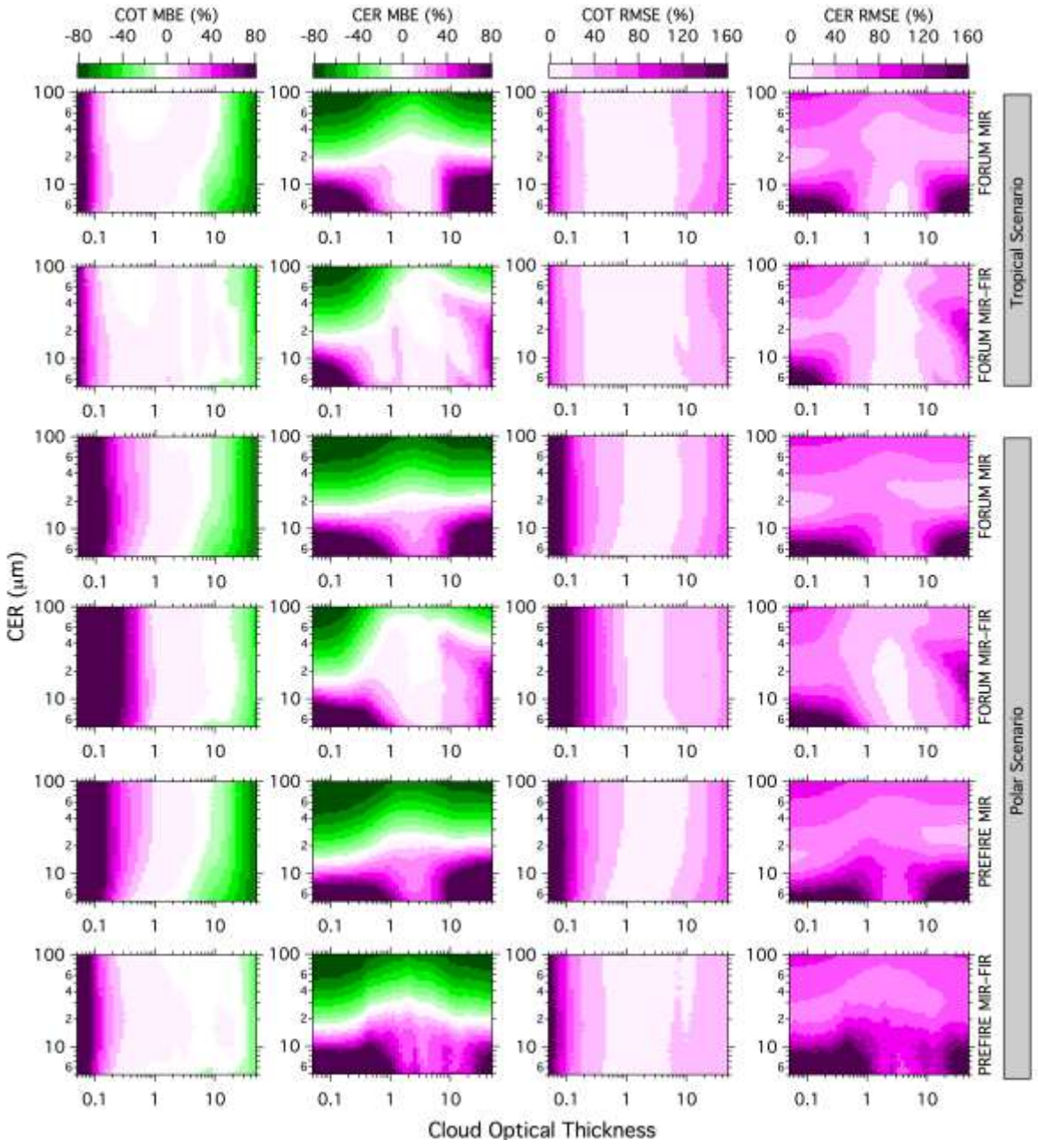

Figure 2. Retrieval error analysis for FORUM-like simulations for both atmospheric scenarios and PREFIRE-like simulations for the polar scenario, for each measurement case. The first and second rows indicate the FORUM-like MIR-based and MIR–FIR-based retrievals for the tropical scenario. The third and fourth rows indicate the counterparts for the polar scenario. The fifth and sixth rows are the same as the third and fourth rows but for PREFIRE-like simulations. In each row, panels show MBEs of (first column) COT and (second column) CER; and RMSEs of (third column) COT and (fourth column) CER.

3.2 Impacts of potential error sources on practical ice cloud retrievals

Figure 3 shows the MBE of the ice cloud property retrievals if the 'real' scene has an ice particle habit or temperature of the ice refractive index which is different from that assumed in the forward model. The results shown are for the FORUM-like MIR–FIR-based retrievals for COT varying from 0.05–50 with CER fixed at 30 μm. The impact of subpixel CFs is also investigated. The retrieval procedure used for the numerical experiment in Section 3.1 is labeled as "Control".

The MBE due to an inconsistent ice particle habit is small for COT retrievals but apparent for CER retrievals across the whole COT range for both atmospheric scenarios. This is because the ice particle habit variation causes a substantial variation in SSA and asymmetry factor (Fig. 1e–f), which are important in terms of radiative transfer calculations for the FIR band signals sensitive to CER. The small COT bias is due to the weak sensitivity of MIR measurements to ice particle habit (Iwabuchi et al., 2014). From the second row of Fig. 3, if there is an inconsistent temperature of the ice refractive index, the bias is small for COT retrievals and is noticeable for CER as implied from the substantial variation of bulk SSA with temperature (Fig. 1b).

253 In the third row of Fig. 3, if the prior subpixel CF information is not available, a typically
254 employed assumption of CF = 100% leads to substantial systematic biases in ice cloud property
255 retrievals for both atmospheric scenarios. The MBE is more substantial for optically thicker clouds,
256 exceeding ±50% for COT >3 when CF is 75%. This indicates that uncertainties of subpixel CF
257 will be one of the major obstacles for ice cloud retrievals using spaceborne MIR–FIR
258 measurements. The last row of Fig. 3 shows that if the prior subpixel CF information is available
259 (e.g., collocated measurements with a fine horizontal resolution), the MBE for non-overcast scenes
260 more closely approaches that from the fully overcast control case. Although the retrieval
261 uncertainty (corresponding to the error bars in Fig. 3) is enhanced due to the contribution of
262 upwelling radiance from the non-cloudy area, the ice cloud property retrievals are feasible even
263 with CF = 50%.
264

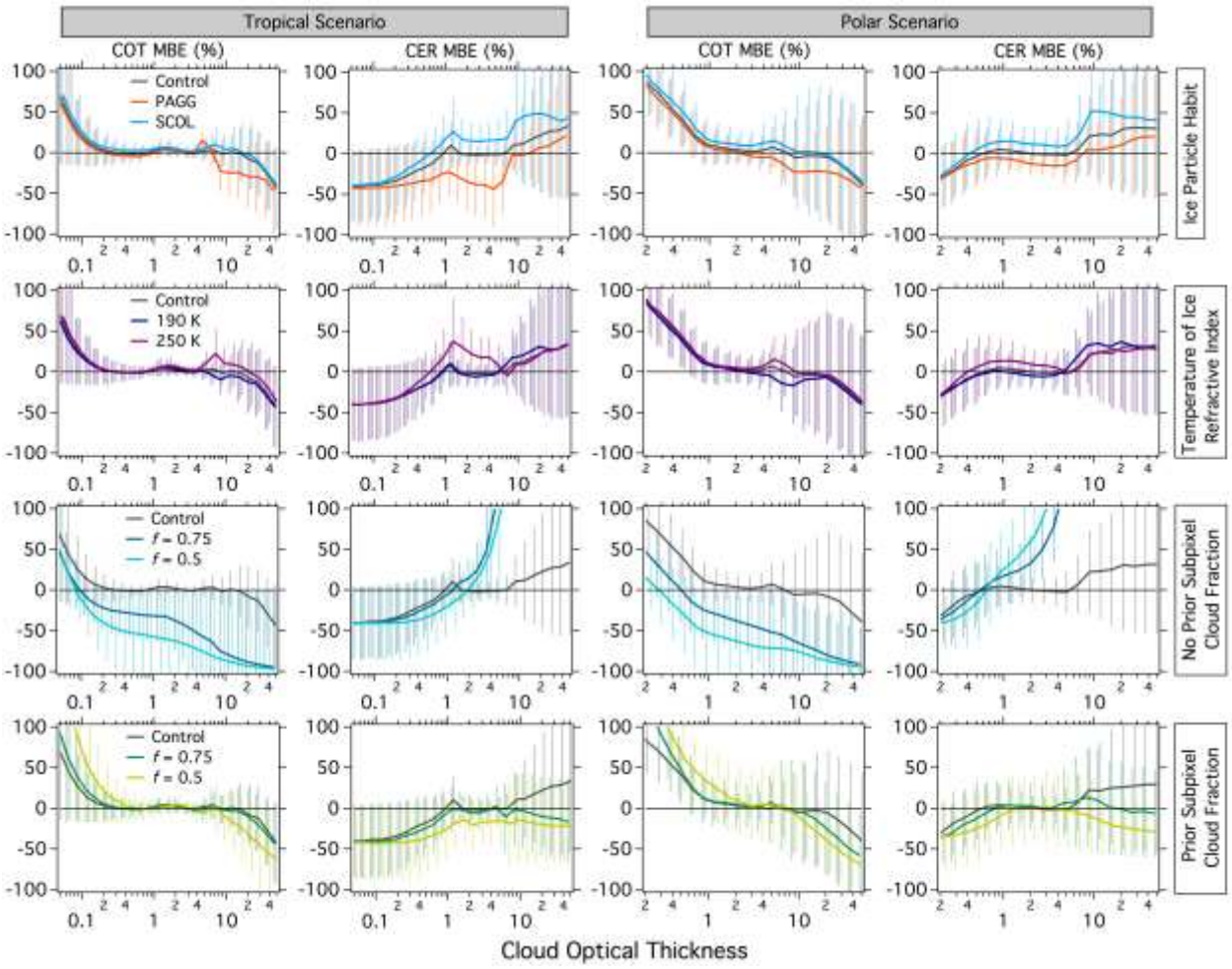

Figure 3. Error analysis for the FORUM-like MIR–FIR-based retrievals in terms of (first row) ice particle habit variations, (second row) temperature variation of ice refractive index, (third row) no prior subpixel CFs (*f*), and (fourth row) prior subpixel CFs. In each row, panels indicate the MBEs of (first column) COT and (second column) CER retrievals for the tropical scenario, and MBEs of (third column) COT and (fourth column) CER retrievals for the polar scenario. The error bars indicate the standard deviation of retrieval error.

4 Conclusions and remarks

We investigated the feasibility of MIR–FIR measurements for ice cloud property retrievals, focusing on the MBE and RMSE of ice cloud property retrievals. Unlike previous studies, the present study takes into account the temperature dependence of the ice refractive index. The MIR–FIR measurements have sufficient sensitivity to ice cloud properties for COT from 0.2–30, which is much wider than the counterpart based on MIR measurements alone, as suggested by Libois and Blanchet (2017).

The subpixel CF critically impacts the quality of the ice cloud property retrievals such that prior information of subpixel CF is essential. Fortunately, such information can be obtained from sensors on operational geostationary satellites in the tropics, and polar-orbiting satellites in polar regions. Prior subpixel CF information substantially reduces systematic retrieval biases based on the MIR–FIR observations.

Neglecting the temperature dependence of ice refractive index can lead to systematic biases in ice cloud property retrievals. The effect of this temperature dependence is more prominent in the FIR than in the MIR. In addition, the single-scattering properties of ice crystals vary with ice particle habit, and cause large biases in CER retrievals when the ice particle habit assumed in the forward modelling is inconsistent with the 'real' particle habit in ice clouds. The vast majority of current ice cloud property retrieval algorithms assume a single ice particle habit. However, as confirmed by previous in-situ and laboratory measurements, the preferred ice particle habits have temperature dependence (e.g., Lawson et al., 2006; Bailey & Hallett, 2009). Therefore, any single ice particle habit model may cause a retrieval bias due to the particle habit variation. Further

investigations of ice particle habit variations are needed to improve an ice particle habit mixture model.

The results here suggest that the MIR–FIR measurements could compensate for the unavailability of VIS–NIR measurements at night. The upcoming two missions, FORUM and PREFIRE, would offer an opportunity to improve nighttime climatological probability density distributions of ice cloud properties. In particular, the FORUM satellite will fly in loose formation with the MetOp-SG-1A satellite deploying the Infrared Atmospheric Sounding Interferometer – New Generation (IASI-NG). Therefore, a synergistic use of robustly accurate MIR spectra from IASI-NG and FIR spectra from FORUM will be expected to further reduce the retrieval uncertainty. However, to fully benefit from this MIR–FIR approach, a pressing need is to develop a more realistic ice particle habit model, including both temperature dependence of ice refractive index and the variation of particle shape with temperature.

Acknowledgments and Data Availability

This work was partly supported by the endowment funds related to the David Bullock Harris Chair in Geosciences (Grant number 02-512231-1000) and internal funds (Grant number 132503-00006) at the College of Geosciences, Texas A&M University. XH is supported by NASA PREFIRE mission program (Grant number 80NSSC18K1485) with a subcontract to the University of Michigan through University of Wisconsin. BHK's contribution was performed at JPL-Caltech under contract with NASA. Data used in this study is archived in the supplemental materials (This will be switched to a public repository, Zenodo https://zenodo.org, upon the acceptance of the manuscript).

References

Bailey, M. P., & Hallett, J. (2009), A comprehensive habit diagram for atmospheric ice crystals: Confirmation from the laboratory, AIRS II, and other field studies. *Journal of the Atmospheric Sciences*, 66(9), 2888–2899.

Bantges, R., Brindley, H. E., Murray, J. E., Last, A. E., Fox, C., Fox, S., Harlow, C., O'Shea, S., Bower, K., Baum, B., Yang, P. and Pickering, J., (2020), A test of the ability of current bulk optical models to represent the radiative properties of cirrus cloud across the mid- and far-infrared, Atmospheric Chemistry and Physics Discussions, doi:10.5194/acp-2019-1181.

Bellisario, C., Brindley, H. E., Murray, J. E., Last, A., Pickering, J., Harlow, R. C., Fox, S., Fox, C., Newman, S. M., Smith, M., Anderson, D., Huang, X., & Chen, X. (2017), Retrievals of the far infrared surface emissivity over the Greenland Plateau using the tropospheric airborne fourier transform spectrometer (TAFTS), *Journal of Geophysical Research: Atmospheres*, 122, 12152–12166, https://doi.org/10.1002/2017JD027328.

Chen, X. H., Huang, X. L., & Flanner, M. G. (2014). Sensitivity of modeled far-IR radiation budgets in polar continents to treatments of snow surface and ice cloud radiative properties. Geophysical Research Letters, 41, 6530– 6537.

Cooper, S. J., & Garrett, T. J. (2010), Identification of small ice cloud particles using passive radiometric observations, *Journal of Applied Meteorology and Climatology*, 49(11), 2334–2347.

Cox, C. V., Harries, J. E., Taylor, J. P., Green, P. D., Baran, A. J., Pickering, J. C., Last, A. E., & Murray, J. E. (2010), Measurement and simulation of mid-and far-infrared spectra in the presence of cirrus, *Quarterly Journal of the Royal Meteorological Society*, 136, 718–739.

Di Natale, G., Palchetti, L., Bianchini, G., & Guasta, M. D. (2017). Simultaneous retrieval of water vapour, temperature and cirrus clouds properties from measurements of far infrared spectral radiance over the Antarctic plateau. *Atmospheric Measurement Techniques*, 10(3), 825–837.

Feldman, D. R., Collins, W. D., Pincus, R., Huang, X., & Chen, X. (2014), Far-infrared surface emissivity and climate, *Proceedings of the National Academy of Sciences of the United States of America*, 111(46), 16297–16302.

Gong, J., Zeng, X., Wu, D. L., & Li, X. (2018). Diurnal variation of tropical ice cloud microphysics: Evidence from Global Precipitation Measurement Microwave Imager polarimetric measurements. *Geophysical Research Letters,* 45, 1185–1193. https://doi.org/10.1002/2017GL075519.

Guillaume, A., Kahn, B. H., Fetzer, E. J., Yue, Q., Manipon, G. J., Wilson, B. D., & Hua, H. (2019), Footprint-scale cloud type mixtures and their impacts on Atmospheric Infrared Sounder cloud property retrievals, *Atmospheric Measurement Techniques*, 12, 4361–4377, https://doi.org/10.5194/amt-12-4361-2019.

Hong, G., Yang, P., Baum, B. A., Heymsfield, A. J., & Xu K.-M. (2009), Parameterization of shortwave and longwave radiative properties of ice clouds for use in climate models, *Journal of Climate.*, *22*(23), 6287–6312.

Hong, Y., Liu, G., & Li, J. F. (2016), Assessing the radiative effects of global ice clouds based on *CloudSat* and *CALIPSO* measurements. *Journal of Climate*, 29, 7651–7674, https://doi.org/10.1175/JCLI-D-15-0799.1.

Huang, X. L., Chen, X. H., Zhou, D. K., & Liu, X. (2016), An observationally based global band-by-band surface emissivity dataset for climate and weather simulations, *Journal of the Atmospheric Sciences*, 73, 3541–3555, doi:10.1175/JAS-D-15-0355.1.

Inoue, T. (1987), A cloud type classification with NOAA 7 split-window measurements, *Journal of Geophysical Research*, 120*92*(D4), 3991–4000.

Iwabuchi, H., Putri, N. S., Saito, M., Tokoro, Y., Sekiguchi, M., Yang, P., & Baum, B. A. (2018). Cloud property retrieval from multiband infrared measurements by Himawari-8. *Journal of Meteorological Society of Japan* Series II, 2018–001. https://doi.org/10.2151/jmsj.2018-001.

Iwabuchi, H., Yamada, S., Katagiri, S., Yang, P., & Okamoto, H. (2014), Radiative and microphysical properties of cirrus cloud inferred from infrared measurements made by the

Moderate Resolution Imaging Spectroradiometer (MODIS). Part I: Retrieval method. *Journal of Applied Meteorology and Climatology*, 53(5), 1297–1316.

Iwabuchi, H., & Yang, P. (2011), Temperature dependence of ice optical constants: Implications for simulating the single-scattering properties of cold ice clouds, *Journal of Quantitative Spectroscopy and Radiative Transfer*, 112(15), 2520–2525, doi:10.1016/j.jqsrt.2011.06.017.

Kahn, B. H., Irion, F. W., Dang, V. T., Manning, E. M., Nasiri, S. L., Naud, C. M., Blaisdell, J. M., Schreier, M. M., Yue, Q., Bowman, K. W., Fetzer, E. J., Hulley, G. C., Liou, K. N., Lubin, D., Ou, S. C., Susskind, J., Takano, Y., Tian, B., & Worden, J. R. (2014), The Atmospheric Infrared Sounder version 6 cloud products, *Atmospheric Chemistry and Physics*, 14, 399–426, https://doi.org/10.5194/acp-14-399-2014.

Kahn, B. H., Schreier, M. M. , Yue, Q., Fetzer, E. J., Irion, F. W., Platnick, S., Wang, C., Nasiri, S. L., & L'Ecuyer, T. S. (2015), Pixel-scale assessment and uncertainty analysis of AIRS and MODIS ice cloud optical thickness and effective radius, *Journal of Geophysical Research: Atmospheres*, 120, doi:10.1002/2015JD023950.

Lawson, R. P., Baker, B., Pilson, B., & Mo, Q. (2006), In situ observations of the microphysical properties of wave, cirrus, and anvil clouds. Part 2: Cirrus clouds. *Journal of the Atmospheric Sciences*, 63, 3186–3203.

Libois, Q., & Blanchet, J.-P. (2017), Added value of far-infrared radiometryfor remote sensing of ice clouds, *Journal of Geophysical Research: Atmospheres*, 122, 6541–6564, doi:10.1002/2016JD026423.

Loeb, N. G., Yang, P, Rose, F. G., Hong, G., Sun-Mack, S., Minnis, P., Kato, S., Ham, S., Smith, W. L., Hioki, S., & Tang, G. (2018), Impact of ice cloud microphysics on satellite cloud retrievals and broadband flux radiative transfer model calculations. *Journal of Climate*, 31, 1851–1864, https:// doi.org/10.1175/JCLI-D-17-0426.1.

Maestri, T., Rizzi, R., Tosi, E., Veglio, P., Palchetti, L., Bianchini, G., Di Girolamo, P., Masiello, G., Serio, C., & Summa, D. (2014), Analysis of cirrus cloud spectral signatures in the far infrared, *Journal of Quantitative Spectroscopy and Radiative Transfer*, 141, 49–64.

Menzel, W. P., Frey, R. A., Zhang, H., Wylie, D. P., Moeller, C. C., Holz, R. E., Maddux, B., Baum, B. A., Strabala, K. I., & Gumley, L. E. (2008), MODIS global cloud-top pressure and amount estimation: Algorithm description and results, *Journal of Applied Meteorology*, 47, 1175–1198, https://doi.org/10.1175/2007JAMC1705.1.

Mlawer, E. J., Turner, D. D., Paine, S. N., Palchetti, L., Bianchini, G., Payne, V. H., et al. (2019). Analysis of water vapor absorption in the far-infrared and submillimeter regions using surface radiometric measurements from extremely dry locations. Journal of Geophysical Research: Atmospheres, 124, 8134–8160. https://doi.org/ 10.1029/2018JD029508.

Mlynczak, M. G., Cageao, R. P., Mast, J. C., Kratz, D. P., Latvakoski, H., & Johnson, D. G. (2016), Observations of downwelling far-infrared emission at Table Mountain California made by the FIRST instrument, *Journal of Quantitative Spectroscopy and Radiative Transfer*, 170, 90–105, doi:10.1016/j.jqsrt.2015.10.017.

Nakajima, T., & King, M. D. (1990), Determination of optical thickness and effective particle radius of clouds from reflected solar radiation measurements. Part 1: Theory. *Journal of the Atmospheric Sciences*, 47, 1878–1893.

Platnick, S., Li, J. Y., King, M. D., Gerber, H., & Hobbs, P. V. (2001), A solar reflectance method for retrieving the optical thickness and droplet size of liquid water clouds over snow and ice surfaces, *Journal of Geophysical Research: Atmospheres*, 106, 15185–15199.

Platnick, S., Meyer, K. G., King, M. D., Wind, G., Amarashinghe, N., Marchant, B., Arnold, G. T., Zhang, Z., Hubanks, P. A., Holz, R. E., Yang, P., Ridgeway, W. L., & Riedi, J. (2017), The MODIS cloud optical and microphysical products: Collection 6 updates and examples from Terra and Acqua, *IEEE Transactions on Geosciences and Remote Sensing*, 55, 502–525, doi:10.1109/TGRS.2016.2610522.

Rathke, C., Fischer, J., Neshyba, S., & Shupe, M. (2002), Improving IR cloud phase determination with 20 microns spectral observations, *Geophysical Research Letters*, 29(8), 501–504, doi:10.1029/2001GL014594.

Ridolfi, M., Del Bianco, S., Di Roma, A., Castelli, E., Belotti, C., Dandini, P., Di Natale, G., Dinelli, B. M., Labonnote, L. C.-, & Palchetti, L. (2020), FORUM Earth explorer 9:

Characteristics of level 2 products and synergies with IASI-NG, *Remote Sensing*, 12, 1496, doi:10.3390/rs12091496.

Rodgers, C. D. (2000), Inverse methods for atmospheric sounding: theory and practice, World Scientific Publishing Co., 238 pp.

Saito, M., Yang, P., Heidinger, A. K., & Li, Y. (2020), An improved beta method for ice cloud property retrievals: Theory, *Journal of Geophysical Research: Atmosphere*, 125, e2019JD031863. https://doi.org/10.1029/2019JD031863.

Sassen, K., Wang, Z., & Liu, D. (2008), Global distribution of cirrus clouds from CloudSat/Cloud–Aerosol Lidar and Infrared Pathfinder Satellite Observations (CALIPSO) measurements, *Journal of Geophysical Research: Atmospheres*, 113, D00A12, doi:10.1029/2008JD009972.

Sekiguchi, M., & Nakajima, T. (2008), A k-distribution-based radiation code and its computational optimization for an atmospheric general circulation model, *Journal of Quantitative Spectroscopy and Radiative Transfer*, *109*(17), 2779–2793.

Stephens, G. L., Tsay, S.-C., Stackhouse Jr, P. W., & Flatau, P. J. (1990), The relevance of the microphysical and radiative properties of cirrus clouds to climate and climatic feedback, *Journal of the Atmospheric Sciences*, 47(14), 1742–1754.

Stubenrauch, C. J., Cros, S., Guignard, A., & Lamquin, N. (2010). A 6-year global cloud climatology from the Atmospheric InfraRed Sounder AIRS and a statistical analysis in synergy with CALIPSO and CloudSat. *Atmospheric Chemistry and Physics*, 10(15), 7197–7214. https://doi. org/10.5194/acp-10-7197-2010.

Turner, D. D., & Mlawer, E. J. (2010). Radiative heating in underexplored bands campaigns (RHUBC). *Bulletin of the American Meteorological Society*, 91(7), 911–924. https://doi.org/10.1175/2010BAMS2904.1

Wan, Z., & Li Z.-L. (1997), A physics-based algorithm for retrieving land-surface emissivity and temperature from EOS/MODIS data, *IEEE Transactions on Geoscience and Remote Sensing*, 35(4), 980–996.

Yang, P., Bi, L., Baum, B. A., Liou, K. N., Kattawar, G. L., Mishchenko, M. I., & Cole, B. (2013), Spectrally consistent scattering, absorption, and polarization properties of atmospheric ice crystals at wavelengths from 0.2 to 100 μm, *Journal of the Atmospheric Sciences*, 70, 330–347.

Yang, P., Mlynczak, M. G., Wei, H., Kratz, D. P., Baum, B. A., Hu, Y. X., Wiscombe, W. J., Heidinger, A., & Mishchenko, M. I. (2003), Spectral signature of ice clouds in the far-infrared region: Single-scattering calculations and radiative sensitivity study, *Journal of Geophysical Research: Atmospheres*, 108(D18), 4569,doi:10.1029/2002JD003291.

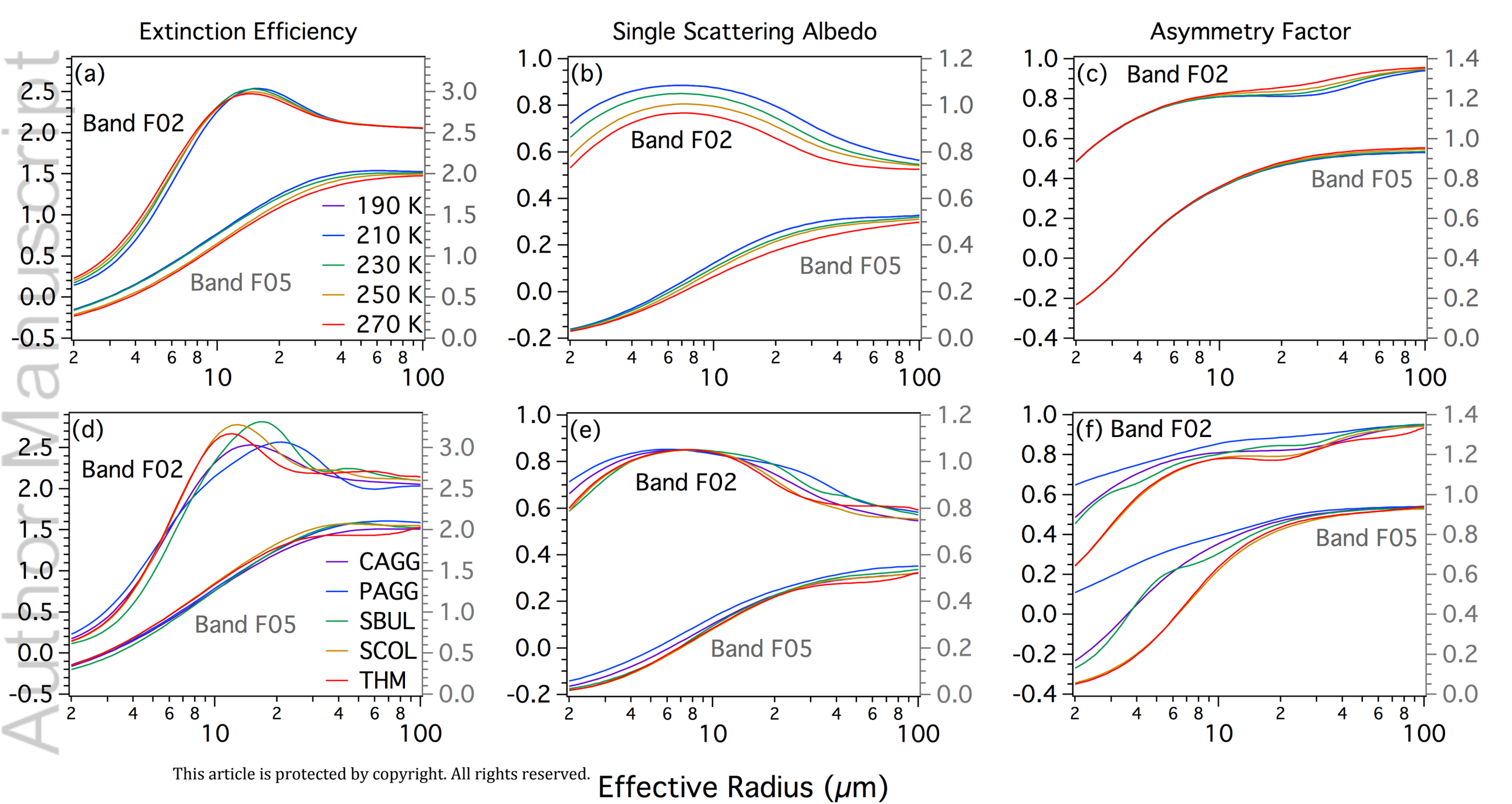

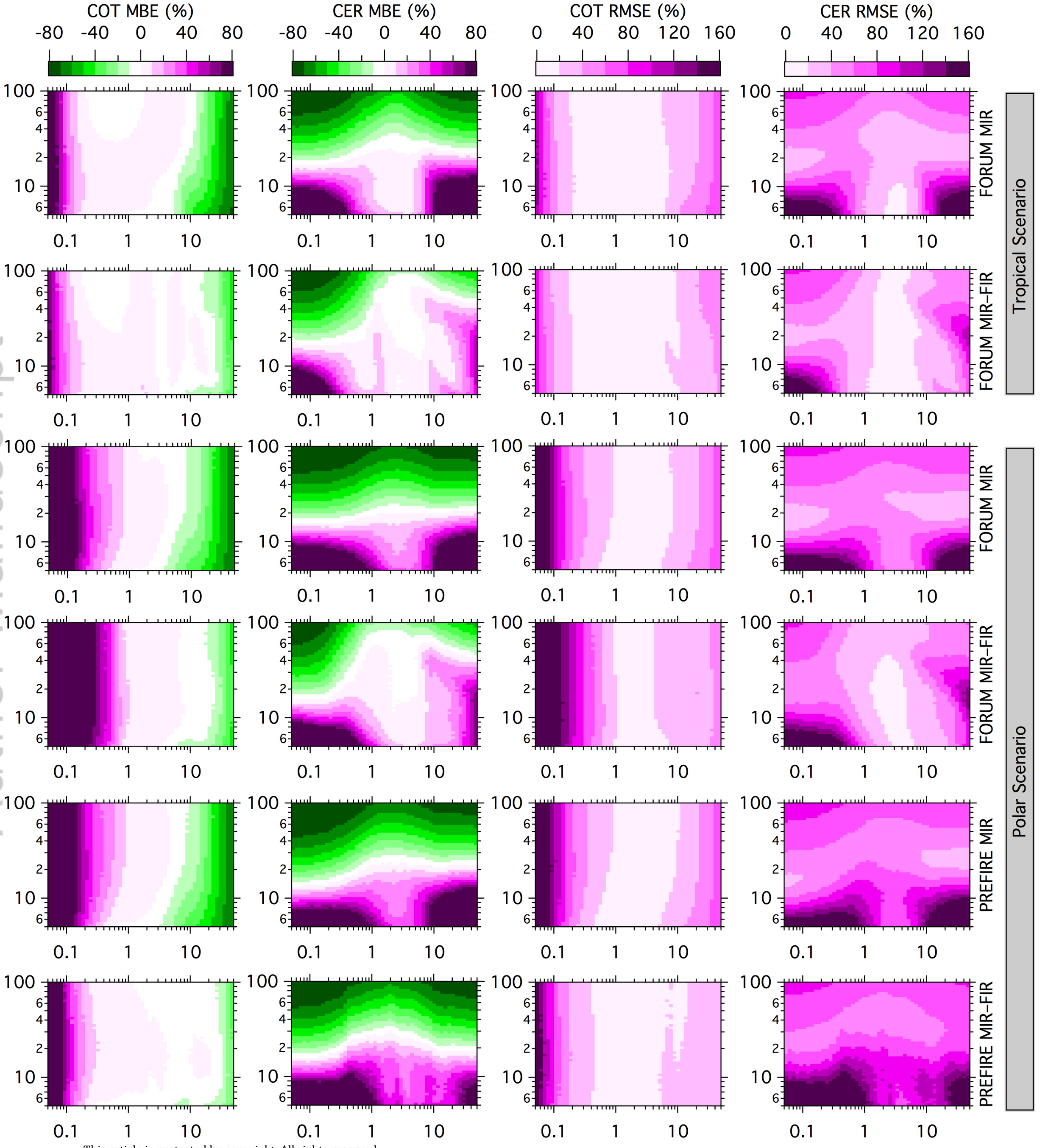

Tropical Scenario

Polar Scenario

COT MBE (%)

CER MBE (%)

COT MBE (%)

CER MBE (%)

Ice Particle Habit

Control
PAGG
SCOL

Temperature of Ice Refractive Index

Control
190 K
250 K

No Prior Subpixel Cloud Fraction

Control
$f = 0.75$
$f = 0.5$

Prior Subpixel Cloud Fraction

Control
$f = 0.75$
$f = 0.5$

100
50
0
-50
-100

0.1
1
10

2 4

Cloud Optical Thickness